Journal of the European Ceramic Society **18** (1998) 185–191

PII: S0955-2219(97)00126-X
0955-2219/98/$19.00 + 0.00

The Physical Properties of Sintered X-phase Sialon Prepared by Silicothermal Reaction Bonding

C. M. Sheppard,* K. J. D. MacKenzie and M. J. Ryan

New Zealand Institute for Industrial Research and Development, PO Box 31-310 Lower Hutt, New Zealand

(Received 13 December 1996; accepted 16 June 1997)

Abstract

A single-step method is described for forming X-phase sialon bodies by silicothermal synthesis from kaolinite, γ-alumina, elemental silicon and 3 wt% Y_2O_3, with simultaneous densification at 1500°C for 8 h. The mechanical properties of this material (Young's modulus, Poisson's ratio, Vickers hardness, strength and fracture toughness) compare well with those of pre-synthesised silicothermal X-phase sialon sintered in a separate step at 1620°C. The mild reaction conditions of the reaction-sintered material are reflected by its microstructure which contains large (50 μm) lath-like X-phase sialon crystals embedded in a matrix of smaller yttrium-containing grains and a few large pores. The mechanical properties of silicothermal X-phase sialon bodies compare favourably with those reported for X-phase bodies sintered at 1650–1720°C and are also comparable with other sialons, silicon nitrides and structurally related aluminosilicate (mullite) ceramics. © *1997 Elsevier Science Limited.*

1 Introduction

X-phase sialon, $Si_{12}Al_{18}O_{39}N_8$, has a structure similar to mullite, and has been synthesised in a number of ways including a novel silicothermal method.[1] From a practical viewpoint, the physical properties of sintered bodies fabricated from these materials are of prime interest, since they dictate their potential applications.

Previously, some physical properties have been reported for X-phase sialon prepared by reaction sintering (hot pressing) both Si_3N_4–Al_2O_3–SiO_2 mixtures and Si_3N_4–mullite gel mixtures at 1650°C[2] and by a two-stage process involving carbothermal synthesis at 1550°C followed by pressureless sintering at 1660–1720°C.[3] The hardness and indentation fracture toughness values for the pressureless sintered bodies were found to be comparable to those of a commercially pure mullite.[3] The hot-pressed material was also reported to be chemically stable in contact with ferrous alloys at 1200°C.[2] Hardness and fracture toughness measurements have also been reported for pressureless sintered composites of mullite with 15 wt% X-phase sialon[4] and indicate an improvement in these properties in the samples containing the sialon. A similar improvement in fracture toughness was found in hot-pressed X-phase sialon composites containing up to 28 vol% of alumina platelets;[5] at higher alumina concentrations, the X-phase sialon was converted to β-sialon.[5]

The X-phase sialon synthesised by our silicothermal method[1] can be fabricated into bodies either by conventional pressureless sintering of compacted pre-synthesised powder at 1620°C, or by single-step pressureless reaction sintering at typically 1500°C. The present paper compares a number of physical properties of sintered bodies fabricated by the two methods with the previously reported properties of other X-phase sialons.

2 Experimental

The starting materials [kaolinite (BDH Chemicals Ltd. 'light'), silicon powder (Permascand 4D) and $Al(OH)_3$ (BDH reagent grade, dehydroxylated at 800°C for 3·5 h)] were batched to X-phase stoichiometry and ball milled in hexane for 20 h using Si_3N_4 milling media. This feedstock was then shaped and sintered in two different ways:

(1) two-step (synthesis + sintering) method (SS)

*To whom correspondence should be addressed.

The solvent was removed from the milled mixture by rotary vacuum evaporator. The resulting powder was mixed to a stiff paste with water, extruded into 5 mm diameter rods, dried and fired in a graphite resistance furnace (Elatec) at 1450°C for 3 h in flowing purified nitrogen (20 litre h^{-1}). The product was ground, then milled with a sintering aid (3 wt% Y_2O_3) in ethanol for 15 h using Si_3N_4 milling media. During the last hour of milling, a binder (4 wt% oleic acid) was added. After milling, the slurry was filtered through 10 μm mesh cloth, the solvent removed by rotary vacuum evaporator and the resulting powder granulated by passing through a 300 μm sieve before uniaxial pressing into 25 mm dia. disks at 300 KPa pressure followed by cold isostatic pressing at 350 MPa. The binder was removed by heating at 5°C^{-1} min to 450°C under flowing nitrogen, and the disks sintered in a graphite resistance furnace (Thermal Technology Inc.) for 1 h at 1620°C under purified nitrogen in a BN powder bed.

(2) Single-step (reaction bonding) method (RB)

The batched starting materials were milled as above with the addition of 2·7 wt% Y_2O_3 to act as a sintering aid; this additive has also been shown to promote the silicothermic formation of X-phase sialon.[1] After solvent removal, the powder was uniaxially pressed into 25 mm dia. disks at 140 KPa pressure, then fired in a horizontal tube furnace at 1500°C for 8 h under purified nitrogen (100 ml min^{-1}).

The disks resulting from the two-step (SS) and one-step (RB) experiments were ground plane parallel using a surface grinder, then polished with 15 μm diamond paste. The polished disk faces were examined by X-ray diffraction (Philips PW 1700 computer-controlled diffractometer with Co Kα radiation and graphite monochromator) and their microstructure examined by scanning electron microscopy with energy dispersive X-ray analysis (SEM/EDX).

The physical properties (density, porosity, Young's modulus, Poisson's ratio, Vickers hardness, fracture toughness and biaxial strength) of the sintered X-phase sialon disks were measured as follows.

The bulk density and open porosity of the samples were measured by water absorption. Both Young's modulus (E) and Poisson's ratio (v) were obtained using an ultrasonic pulse-echo method[6] in which measurements are made of the acoustic velocity of ultrasound in the material:

$$E = 4\rho\left[\{\tfrac{3}{4}C_l^2 - C_t^2\}/\{(C_l/C_t)^2 - 1\}\right] \quad (1)$$

$$\nu = \left[\frac{1}{2}(C_l^2 - C_t^2)\right]/(C_l^2 - C_t^2) \quad (2)$$

where ρ is the density of the material and C_l and C_t are respectively the longitudinal and transverse ultrasound velocities.

The hardness measurements were made using a Vickers diamond pyramidal indenter with a load of 5 kg and are reported as the average of five indentations. The indentation dimensions and crack lengths were measured from SEM micrographs.

Detailed SEM examination of the cracking behaviour in the vicinity of the Vickers indentations indicated typical halfpenny cracks. The values of the fracture toughness K_{IC} were therefore calculated from the SEM crack length measurements using the relationship[7]

$$K_{IC} = 0{\cdot}016(E/H)^{1/2}P/c^{3/2} \quad (3)$$

where E is the elastic modulus, H is the hardness, P is the indentation load and c is the radial crack length.

Biaxial strength measurements were determined by the 'ball on ring' (BOR) method in which the specimen is supported by a circular ball-bearing race and loaded centrally with a ball. The equibiaxial stress, σ, at the centre is given[8] by

$$\sigma = [3P(1+\nu)/4\pi t^2]\{1 + 2[\ln(a/b)] + [(1-\nu)a^2/(1+\nu)R^2][1 - (b^2/2a^2)]\} \quad (4)$$

where P is the breaking load, t and R are the sample disk thickness and radius, respectively, a is the radius of the support ring, b is the radius of the central loading region (taken as t/3) and ν is Poisson's ratio, determined ultrasonically as above. The circular specimens were supported on a 16·89 mm diameter ring and broken using an Instron 1122 Universal Testing Machine at a crosshead speed of 0·1 mm min^{-1}.

The Al/Si ratios of the sintered discs were determined using a Link Isis system (Oxford Instruments) mounted on a Cambridge Stereoscan 250 Mk 2 scanning electron microscope. Quantitation was obtained using aluminium metal and albite standards.

3 Results and Discussion

The X-ray diffraction patterns from the polished faces of the SS (two-step sintered) and RB (single-step sintered) disks are shown in Fig. 1(A) and (B), respectively.

Figure 1(A) shows the two-step product contains essentially monophase crystalline X-phase sialon with all the expected X-phase sialon reflections present in this pattern, and no additional lines to suggest the presence of any other crystalline phase. The XRD pattern of the one-step sintered (RB) sample [(Fig. 1(B)] indicates, in addition to crystalline X-phase sialon, a small amount of O'-sialon, probably arising from the presence of yttria during the synthesis stage (yttria promotes the formation of both X-phase[1] and O'-sialon[9]). Guinier X-ray photographs of powdered SS material gave the following cell parameters for silicothermally synthesised X-phase sialon: a = 9·669(1)Å, b = 8·5438(5)Å, c = 11·189(1)Å, $\alpha = 90{\cdot}000(8)°$, $\beta = 124{\cdot}370(8)°$, $\gamma = 98{\cdot}458(6)°$. These cell dimensions are in good agreement with published values from a single-crystal X-ray structural study.[10] No crystalline yttrium-containing phases are detectable in either the SS or the RB samples, but the latter seems slightly more crystalline than the former.

Scanning electron micrographs of the SS and RB sintered samples are shown in Fig. 2(A) and (B), respectively.

The SS disk produced by two-step sintering shows some closed porosity [(Fig. 2(A)], most of the pores being very small and only a few larger pores evident. Although XRD suggests the sample contains only X-phase and some glass, the micrographs show the presence of at least two morphologies. According to EDX, the darker grey crystals, about 20 μm in length, contain only Si, Al, O and N, and all indicate an Al/Si ratio close to 2·0; this composition is not consistent with the targeted composition (Al/Si = 1·5), but agrees with the X-phase composition $Si_{12}Al_{24}O_{48}N_8$ found by Thompson and Korgul[10] and suggested by Bergman *et al.*[11] to represent one end-point of the solid solubility range for this phase. The lower Si content of the product by comparison with the starting mix suggests the formation of volatile SiO during the reaction. The lighter grey matrix areas interspersed with small, brighter spots are also of X-phase composition but with generally slightly higher Al content (Al/Si ratios typically 1·7–1·9). The matrix areas also contain the yttrium (1·2–2·2 atomic %), possibly residing in the brighter spots which are however too small to be individually

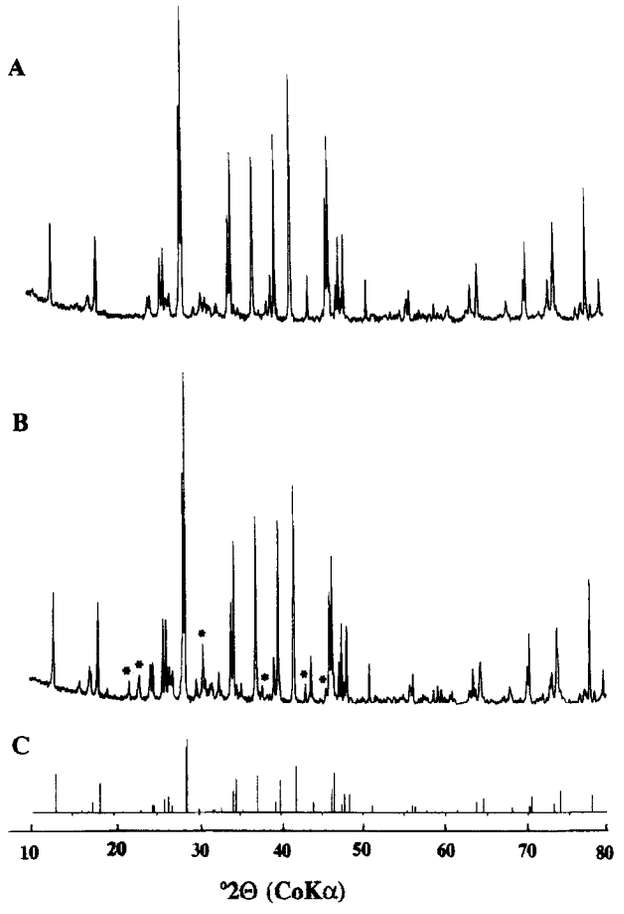

Fig. 1. Typical XRD patterns from sintered X-phase sialon discs prepared by silicothermal synthesis. (A) Two-step sintered (SS) sample. (B). Single-step (RB) sample. C. ICDD data file No. 36-832 for X-phase sialon. Asterisks indicate O'-sialon impurity (ICDD file No. 42-1492)

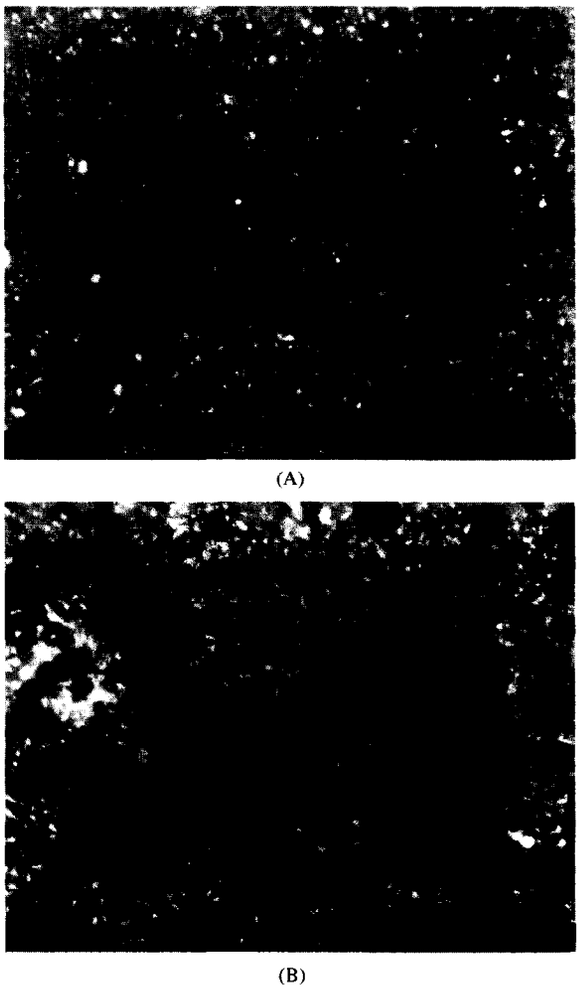

Fig. 2. Backscattered electron scanning micrographs of typical areas of sintered silicothermal X-phase sialon bodies. (A). Two-step sintered (SS) sample. (B). Single-step (RB) sample.

probed by the SEM electron beam. If any discrete Y-containing phases are present, they are either too glassy or present in insufficient concentrations to be detected by XRD.

The RB disks (one-step sintered) show slightly more large pores [(Fig. 2(B)] but fewer if any very small pores by comparison with the SS disks. The X-phase sialon crystals, which show up as darker grey, have identical Al/Si ratios to those in the SS samples, but are of larger size (up to 50 μm), consistent with XRD evidence of increased crystallinity. As in the SS samples, the lighter grey matrix material is slightly richer in Si (Al/Si = 1·85–1·96), and contains the yttrium, possibly in the brighter spots. A few larger bright areas at the rims of the large pores show even higher Si and Y contents, suggesting that yttrium silicate glass may be implicated in pore formation.

The larger X-phase sialon crystallite size in the RB disks probably reflects the longer sintering time of these samples. The greater pressing pressure and higher sintering temperature experienced by the SS samples accounts for the smaller size of pores found in these disks.

Figure 3 shows the distribution of aluminium, silicon and yttrium in a single area of an RB sintered disk, mapped by EDX without background subtraction.

The Al and Si maps confirm that the ratio of Si to Al is essentially constant throughout the sample, except in some areas in the vicinity of pores which are enriched in Si [(Fig. 3(D)] and depleted in Al [(Fig. 3(C)]. The distribution of Y varies [(Fig. 3(B)], being depleted in the large lath-like X-phase crystals and residing principally in the matrix.

The mechanical properties determined for X-phase sialon disks produced by the RB and SS methods are summarised in Table 1, which also includes for comparison a selection of the available literature values for X-phase sialon bodies, other sintered sialons and related materials.

3.1 Density, porosity and shrinkage

Table 1 indicates that comparable densities are produced by both sintering methods, which also produce no open porosity. The densities are consistent with the value reported[3] for carbothermally

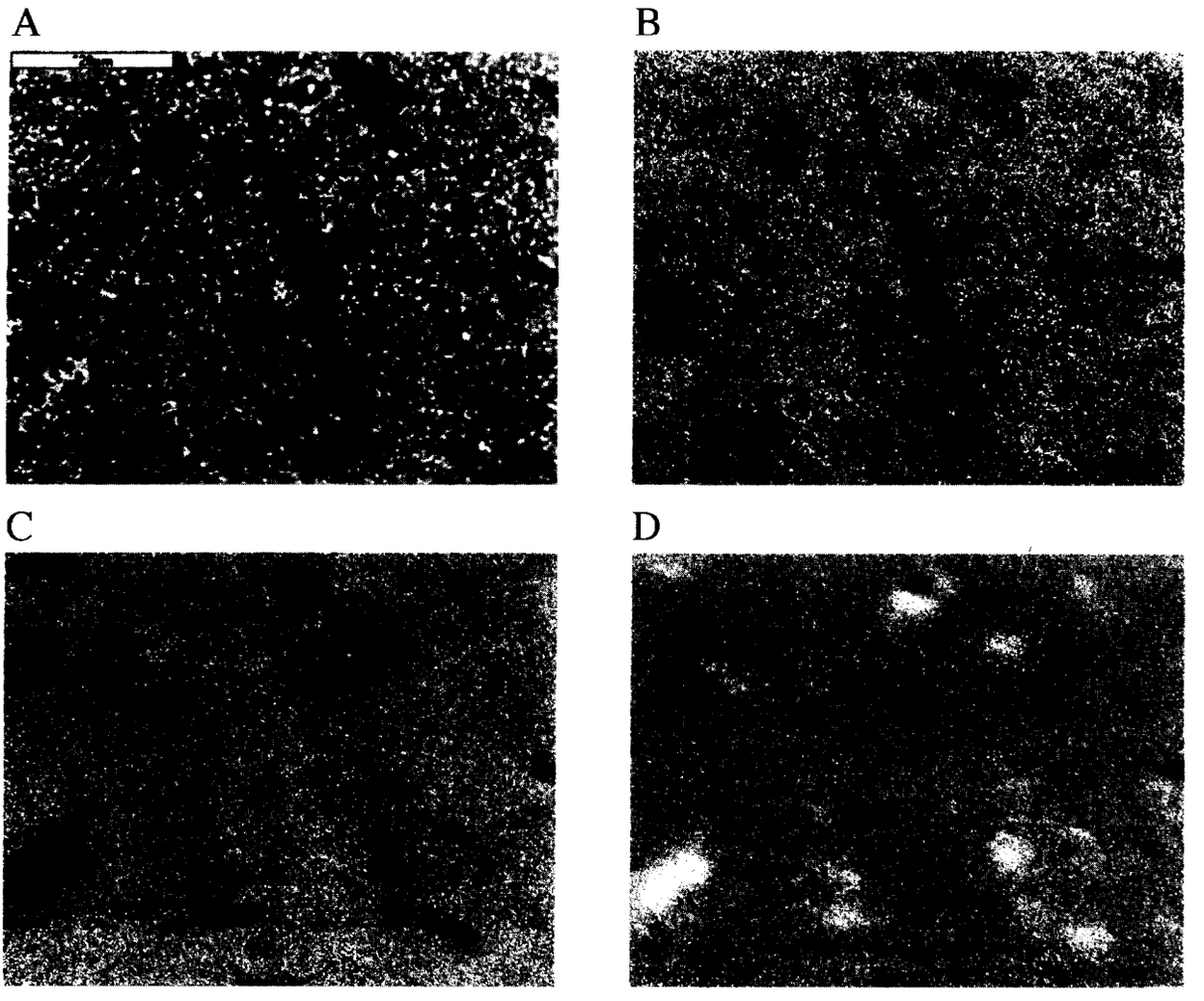

Fig. 3. EDX elemental distribution maps of a typical RB sintered silicothermal X-phase sialon body. (A) Backscattered electron image, (B) Y map, C. Al map, D. Si map

Table 1. Properties of RB and SS sintered X-phase sialon (this work) with literature values for properties of related materials (references in parenthesis)

Material	*Density (g cm^3)*	*Poisson's ratio*	*Young's modulus (GPa)*	*Vickers hardness (GPa)*	*Strength (MPa)*	*Fracture toughness (MPa m$^{1/2}$)*
X-phase (RB)	3·004 ± 0·004	0·264 ± 0·002	206 ± 1	15 ± 1	233 ± 25[e]	1·4 ± 0·1
X-phase (SS)	3·054 ± 0·003	0·265 ± 0·008	217 ± 3	12 ± 1	253 ± 8[e]	1·05 ± 0·08
X-phase	3·01–3·04 (2,3)	—	213 (2)	12·5–12·8 (2)	—	1·17–1·76 (2)
				10·4–11·1 (3)		3·1–3·3 (3)
Si_3N_4[f]	1·8–2·7 (12)	0·2 (19)	120–220 (20)	10·0–12·0 (12)	150–350 (20)	1·5–2·8 (20)
β-sialon[a]	3·08–3·2 (13)	0·29–0·3 (14)	100–180 (13)	13–15 (13)	364–450 (13)	2·0–3·8 (13)
	3·1 (14)		218–221 (14)	14–14·9 (14)	378–452[e] (14)	2·5–3·1 (14)
α-sialon[b]	3·15–3·3 (15,16)	—	—	19[g] (16)	458–580 (15)	2·7–3·3[g] (16)
				23·5 (22)	530 (22)	3·6 (22)
				20·5 (23)	600 (23)	4·3 (23)
O-sialon[c]	2·80[f] (17)	0·17[f] (17)	218–223[f] (17)	15[g] (9)	424[f] (17)	3·5[g] (9)
Si_2N_2O[d]	2·83 (18)	0·19–0·2 (18)	222 (23)	15·8 (19)	250 (18)	4·4 (18)
Mullite	2·8 (19)	0·25 (19)	145 (19)	11·6 (3)	185 (19)	2·2 (19)
	3·01–3·05 (21)		195–202 (24)		180–220 (21)	2·3–2·5 (21)

[a] FZor a range of z-values from ≈0 to 4·27.
[b] Y-sialon, x = 0·45.
[c] x = 0·22.
[d] Contains 5 wt% MgO as a sintering aid.
[e] Determined by the ball-on-ring method.
[f] Reaction bonded, pressureless sintered.
[g] Hot isostatically pressed.

synthesised X-phase sialon (3·01 g cm^{-3}) (Table 1). Although both SS and RB samples register zero porosity to liquid absorption, the SEM results indicate that each contains a degree of closed porosity. The slightly higher density of the SS disks may reflect the smaller pore size resulting from higher pressing pressures and sintering temperatures. Since the RB sintering process is carried out at lower temperatures, the sintering time must be sufficiently long to permit full densification. This is illustrated by experiments using sintering times ranging from 4 to 8 h at 1500°C, during which time the density increased from 2·99 to 3·01 g cm^{-3} and the open porosity decreased from 0·63 to 0%. Sintering for 2 h at 1550°C produced slightly lower open porosity but lower density than sintering for 6 h at 1500°C, suggesting that the higher temperature produces pore closure rather than pore elimination.

The measured shrinkage in going from the green state to full fired density is less in the SS than in the RB samples (24·5 and 30·0%, respectively). It is not possible to decrease the shrinkage in the latter by increasing the pressing pressure prior to firing because the green disk must have sufficient porosity to allow the penetration of the nitrogen gas necessary for the RB process. Since the nitridation of the silicon is complete by 1380°C (Fig. 4), any sintering of the disks which may occur above this temperature should have no further effect on the formation of X-phase sialon, which proceeds in tandem with the sintering process (Fig. 4).

3.2 Mechanical properties

Table 1 shows that the mechanical properties of samples produced by RB and SS processes are comparable. The slightly higher values of Young's modulus and strength of the SS samples possibly result from the higher pressing pressure and sintering temperature. The mechanical properties are comparable with the reported values for sintered X-phase samples (Table 1), with the exception of the unusually high fracture toughness values of Anya and Hendry.[3] The comparable mechanical properties of the RB samples clearly establish the usefulness of this method for fabricating robust samples at lower temperatures and milder conditions than the conventional SS method.

In comparing these properties with those listed in Table 1 for other sialons and for the structurally related aluminosilicate mullite, it must be

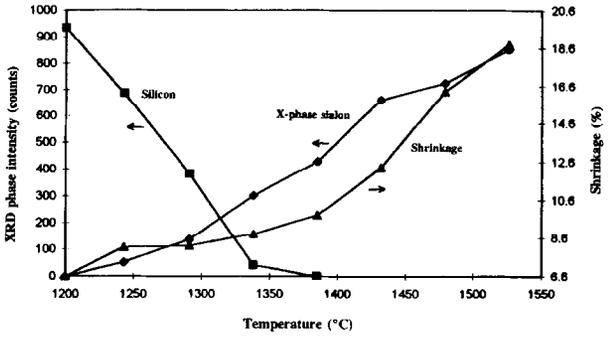

Fig. 4. Intensity of the major XRD reflections of X-phase sialon and elemental Si together with shrinkage of fired body as a function of heating temperature during sintering of a single-step (RB) silicothermal disk

remembered that these values are strongly influenced both by the sample parameters (composition, structure, fabrication method and previous history) and by the test method. Nevertheless, the typical values collected in Table 1 indicate that the present X-phase sialon produced by silicothermal synthesis and sintered by both the SS and RB processes compares favourably with reaction-bonded silicon nitride and mullite but is inferior to the Vickers hardness and fracture toughness of β-sialon and silicon oxynitride and to the hardness, strength and fracture toughness of a typical α-sialon (Table 1). It has been reported[13] that for a series of β-sialons of differing composition, Young's modulus, Vickers hardness and strength all decrease regularly with increasing Al content; the fracture toughness also changes, but in a non-linear manner, with Al content. A similar dependence on Al content may be suggested for the Young's modulus, Vickers hardness and strength values of the present X-phase samples which are all slightly superior to those of the isostructural aluminosilicate phase mullite in which the Al/Si ratio is up to twice that of X-phase sialon (3·0 and 1·5–2·0 respectively), but are slightly inferior to sialons containing less Al (β-sialon with $z = 0{\cdot}5$–3·0, O'-sialon with $x = 0{\cdot}2$ and Si_2N_2O, in which the Al/Si ratio is 0·09–1·0, 0·1 and 0, respectively). These factors are less important in determining the mechanical properties of the α-sialons, in which the excellent hardness and strength is related to the microstructure and intergranular chemistry, which enables the hard, equiaxed grains to bond with minimal formation of weaker glassy phases; this gives α-sialon an advantage over X-phase and other monophase sialons.

Nevertheless, the present results suggest that useful applications may be found for SS and RB X-phase sialon, both in their own right and as a component of sialon-based composite materials.

4 Conclusions

X-phase sialon bodies have been prepared by silicothermal synthesis and densified by two sintering procedures. The two-step higher-temperature process produces bodies at 1620°C with small X-phase grains and small closed pores. Comparable densities close to theoretical can be obtained using a single-step reaction sintering process at 1500°C with a longer holding time (8 h) which gives larger X-phase sialon grains. The 3 wt% Y_2O_3 which is added as a sintering aid in both cases is distributed within the fine-grained matrix.

The mechanical properties (Young's modulus, Poisson's ratio, Vickers hardness, strength and fracture toughness) of X-phase sialon bodies sintered by both methods are comparable with those previously reported for X-phase sialon prepared by carbothermal synthesis at higher temperatures (1600–1720°C), and with reaction bonded Si_3N_4 and structurally-related mullite. Thus, the low-temperature sintering methods show promise for the fabrication of practical materials based on X-phase sialon.

Acknowledgement

We are indebted to K. Card for the scanning electron microscopy.

References

1. Sheppard, C. M., MacKenzie, K. J. D., Barris, G. C. and Meinhold, R. H., A new silicothermal route to the formation of X-phase sialon: the reaction sequence in the presence and absence of Y_2O_3. *Journal of the European Ceramic Society*, 1997, **17**, 667–673.
2. Zhou, Y., Vleugels, J., Laoui, T., Ratchev, P. and Van der Biest, O., Preparation and properties of X-sialon. *J. Mater. Sci.*, 1995, **30**, 4584–4590.
3. Anya, C. C. and Hendry, A., Hardness, indentation fracture toughness and compositional formula of X-phase sialon. *J. Mater. Sci.*, 1994, **29**, 527–533.
4. Anya, C. C. and Hendry, A., Sintering, hardness and indentation fracture toughness (K_{IC}) of mullite and its composite with 15 wt% X-phase sialon. *Journal of the European Ceramic Society*, 1994, **13**, 247–256.
5. Zhou, Y., Vleugels, J., Laoui, T. and Van der Biest, O., Toughening of X-sialon with Al_2O_3 platelets. *Journal of the European Ceramic Society*, 1995, **15**, 297–305.
6. Krautkrämer, J. and Krautkrämer, H., *Ultrasonic Testing of Materials*, 2nd revised German edn, Springer-Verlag, Berlin/Heidelberg, 1969, pp. 464–465.
7. Anstis, G. R., Chantikul, P., Lawn, B. R. and Marshall, D. B., A critical evaluation of indentation techniques for measuring fracture toughness: I. Direct crack measurements. *J. Amer. Ceram. Soc.*, 1981, **64**, 533–538.
8. de With, G. and Wagemans, H. H. M., Ball-on-ring test revisited. *J. Amer. Ceram. Soc.*, 1989, **72** 1538-1541.
9. Ekström, T., Olsson , P.-O. and Holmström, M., O'-sialon ceramics prepared by hot isostatic pressing. *Journal of the European Ceramic Society*, 1993, **12**, 165–176.
10. Thompson, D. P. and Korgul, P., Sialon X-phase. In *Progress in Nitrogen Ceramics*, ed. F. L. Riley. Martinus Nijhoff Boston, 1983, pp. 375–380.
11. Bergman, B., Ekström, T. and Micksi, A., The Si–Al–O–N system at temperatures of 1700–1775°C. *Journal of the European Ceramic Society*, 1991, **8**, 141–151.
12. Parr, N. L. and May, E. R. W., The technology and engineering applications of reaction-bonded Si_3N_4. *Proc. Brit. Ceram. Soc.*, 1967, **7**, 81–98.
13. Glauckler, L. J., Prietzel, S., Bodemer, G. and Petzow, G., Some properties of β-$Si_{6-x}Al_xO_xN_{8-x}$. In *Nitrogen Ceramics*, ed. F. L., Riley, Noordhoff, Leyden, 1977, pp. 529–538.
14. Kokmeijer, E, de With, G. and Metselaar, R., Microstructure and mechanical properties of β'-$Si_3Al_3O_3N_5$ ceramics. *Journal of the European Ceramic Society*, 1991, **8**, 71–80.
15. Mitomo, M., Tanaka, H., Muramatsu, K., Li, N. and Fujii, Y., The strength of α-sialon ceramics. *J. Mater. Sci.*, 1980, **15**, 2661–2662.

16. Bartek, A., Ekström, T., Herbertsson, H. and Johansson, T., Yttrium α-sialon ceramics by hot isostatic pressing and post-hot isostatic pressing. *J. Amer. Ceram. Soc.*, 1992, **75**, 432–439.
17. Barris, G. C., Brown, I. W. M., Ekström, T. C, White, G. V., Cooper, M. and Hodren, G. M., O'-sialon-silicon carbide refractories for use in the aluminium industry. *Proc. IPENZ Ann. Conf.*, 1996, **2**, 319–324.
18. Boch, P. and Glandus, J. C., Elastic properties of silicon oxynitride. *J. Mater. Sci.*, 1979, **14**, 379–385.
19. Bauccio, M. (ed), *Engineering Materials Reference Book*, 2nd edn. ASM International, Ohio, 1994, p. 210.
20. Zeigler, G., Heinrich, J. and Wötting, G., Relationship between processing, microstructure and properties of dense and reaction-bonded silicon nitride. *J. Mater. Sci.*, 1987, **22**, 3041–3086.
21. Osendi, M. I. and Baudin, C., Mechanical properties of mullite materials. *Journal of the European Ceramic Society*, 1996, **16**, 217–224.
22. Sheu, T-Z., Microstructure and mechanical properties of the in situ β-Si_3N_4/α'-sialon composite. *J. Amer. Ceram. Soc.*, 1994, **77**, 2345–2353.
23. Hwang, S-L, Lin, H-T. and Becher, P. F., Mechanical properties of β-Si_3N_4 whisker reinforced α'-ceramics. *J. Mater. Sci.*, 1995, **30**, 6023–6027.